

# Magnetoresistance and planar Hall effects in submicron exchange-coupled NiO/Fe<sub>19</sub>Ni<sub>81</sub> wires

A. Nemoto, Y. Otani,<sup>a)</sup> S. G. Kim, and K. Fukamichi

Department of Materials Science, Graduate School of Engineering, Tohoku University, Aoba 02,  
Sendai 980-8579, Japan

O. Kitakami and Y. Shimada

Research Institute for Scientific Measurements, Tohoku University, Sendai 980-8577, Japan

(Received 14 December 1998; accepted for publication 23 February 1999)

Magnetization reversal processes of submicron NiO/Fe<sub>19</sub>Ni<sub>81</sub> exchange-coupled Hall cross with a variable width in the range from 0.2 to 0.4  $\mu\text{m}$  were studied by the magnetoresistivity and the planar Hall effect measurements. The magnetization reversal was found to take place via a coherent rotation in the Hall cross, suggesting that the size of the antiferromagnetic domain is regulated by the wire width. The magnitude of the exchange coupling field  $H_{\text{ex}}$  varied in proportion to the inverse wire width. © 1999 American Institute of Physics. [S0003-6951(99)02116-6]

The unidirectional magnetic anisotropy caused by the interfacial exchange coupling between antiferromagnetic (AF) and ferromagnetic ( $F$ ) layers governs a shift of the magnetic hysteresis loop along the magnetic field axis, known as the exchange-coupling field  $H_{\text{ex}}$ . Since this phenomenon can be utilized for controlling the magnetization direction of a ferromagnetic layer in spin valve structures, extensive studies have been carried out on various exchange-coupled bilayers such as NiMn/Fe-Ni,<sup>1</sup> Cr-Al/Fe-Ni,<sup>2</sup> and NiO/Fe-Ni.<sup>3</sup>

The value of  $H_{\text{ex}}$  is usually two or three orders of magnitude smaller than that expected from the interatomic exchange coupling. In order to explain this discrepancy, several models have been proposed. Mauri *et al.*<sup>4</sup> first suggested that the unidirectional anisotropy energy is provided by the energy of the AF domain wall formed at the AF/ $F$  interface when the magnetization of the  $F$  layer is reversed. Malozemoff<sup>5</sup> then applied the random field approximation to take into account the atomic scale interface roughness, and found that the antiferromagnetic domain size is closely related to the  $H_{\text{ex}}$ . Recently Koon<sup>6</sup> presented numerical calculations for the AF/ $F$  bilayer with compensated ferromagnetic and antiferromagnetic interfaces. The model explained various experimental results such as high field rotational hysteresis<sup>7</sup> and positive exchange field.<sup>8</sup> These models commonly suggested that the domain wall formation or the domain structure in the antiferromagnetic layer significantly affects the magnetic properties of the exchange-coupled bilayers.

In the present study, we prepared the submicron scale exchange-coupled NiO/Fe<sub>19</sub>Ni<sub>81</sub> wires with a variable width from 0.2 to 0.4  $\mu\text{m}$  by microfabrication techniques to investigate the effect of the exchange coupling area on the field  $H_{\text{ex}}$ . Magnetoresistance measurements and planar Hall measurements were, for the first time, employed to evaluate the magnetization process in the small exchange coupled region.

Wire structures with current and voltage leads were pat-

terned on a Si substrate with a 3000 Å positive resist layer by means of electron-beam lithography. A NiO film with a thickness of 1000 Å was then deposited by a rf magnetron sputter method. A Fe<sub>19</sub>Ni<sub>81</sub> film with a thickness of 200 Å was deposited on top of the NiO film by a dc magnetron sputter method. The base pressure was  $2 \times 10^{-7}$  Torr and Ar pressure during the deposition was 4 mTorr for both films. A magnetic field of 550 Oe was applied during the entire deposition process. Finally, a lift-off process completes the exchange-coupled small structure as shown in Fig. 1(a).

The detailed structure is shown in Fig. 1(b). The wire width was varied from 0.2 to 0.4  $\mu\text{m}$  and the width of the voltage leads were fixed at 0.5  $\mu\text{m}$ . The wire axis was directed parallel to the induced unidirectional anisotropy direction. Since the wire was too small to carry out magnetization

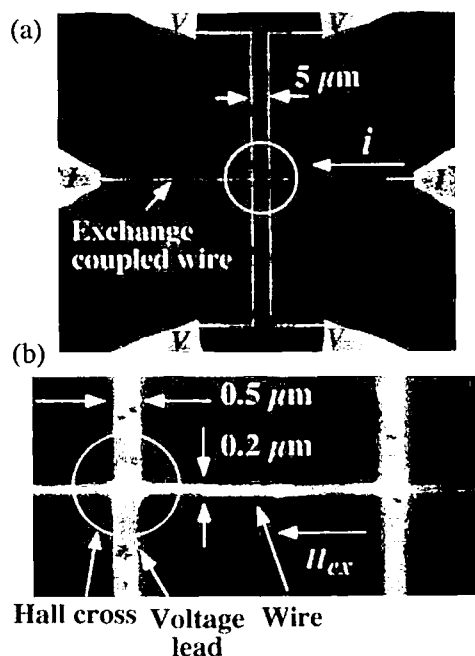


FIG. 1. (a) Scanning electron micrograph of an exchange-coupled NiO/Fe<sub>19</sub>Ni<sub>81</sub> wire; (b) a magnified image in a measurement area.

<sup>a)</sup>Author to whom correspondence should be addressed; electronic mail: chika@material.tohoku.ac.jp

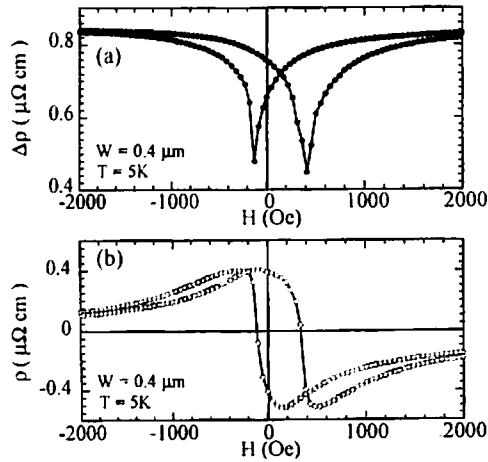


FIG. 2. The magnetoresistance curve (a) and the planar Hall resistance curve (b) measured at 5 K for a NiO/Fe<sub>19</sub>Ni<sub>81</sub> exchange coupled wire 0.4 μm in width.

measurements, magnetotransport measurements were employed to evaluate the local magnetic state of the wire. The magnetization process in the Hall cross was investigated by planar Hall effect measurements, while the magnetization process in the wire was studied by magnetoresistance effect measurements. Both measurements were performed by an ac four terminal method in the temperature range from 5 to 300 K in fields from -10 to 10 kOe. The magnetic fields were applied parallel to the current in the film plane.

Figures 2(a) and 2(b), respectively, show a magnetoresistivity and planar Hall resistivity curves measured at 5 K for a NiO/Fe<sub>19</sub>Ni<sub>81</sub> exchange coupled wire 0.4 μm in width. Both curves exhibit large shifts of hysteresis loops along the magnetic field axis. The value of  $H_{ex}$  evaluated as the shift is about 150 Oe, which is larger than 115 Oe of a bilayer film prepared under the same condition. The magnetic hysteresis loops were then calculated from the obtained planar Hall resistivity and magnetoresistivity curves as follows. The electric field in the magnetic materials can be written as  $\mathbf{E} = \rho_{\perp} \mathbf{j} + (\rho_{\parallel} - \rho_{\perp}) \mathbf{m}(\mathbf{j} \cdot \mathbf{m})$ , where  $\mathbf{j}$  is the current density vector,  $\mathbf{m}$  is the unit magnetization vector, and  $\rho_{\parallel}$  and  $\rho_{\perp}$  are the saturation resistivities perpendicular and parallel to  $\mathbf{j}$ .<sup>9</sup> When the current  $\mathbf{j}$  is parallel to the wire axis, the magnetoresistivity  $\rho_x$  and the planar Hall resistivity  $\rho_y$  are, respectively, deduced as  $\rho_x = \rho_{\perp} + (\rho_{\parallel} - \rho_{\perp}) \cos^2 \theta$  and  $\rho_y = (1/2)(\rho_{\parallel} - \rho_{\perp}) \sin^2 \theta$ , where  $\theta$  is the angle between  $\mathbf{j}$  and  $\mathbf{m}$ . Magnetic hysteresis loops calculated from the above relations are shown in Fig. 3. The shapes of both hysteresis loops are quite different, indicating that the magnetization reversal is more difficult in the wire than in the cross. The magnetization reversal initially occurs in the cross followed by a sharp magnetization reversal in the wire.

For comparison, the magnetization reversal processes were numerically simulated as shown in Fig. 4. The cross region was divided into five segments with a single domain structure as shown in the inset of Fig. 4(a). The magnetostatic energies were evaluated from the wire width  $W$  and  $\theta$  as  $-4M_F^2 t_F \cos^2 \theta / W$ , where  $M_F$  and  $t_F$  are the magnetization and thickness of the ferromagnet. The ferromagnetic exchange coupling strength between neighboring single domain  $i, j$  segments was approximated as  $J \cos(\theta_i$

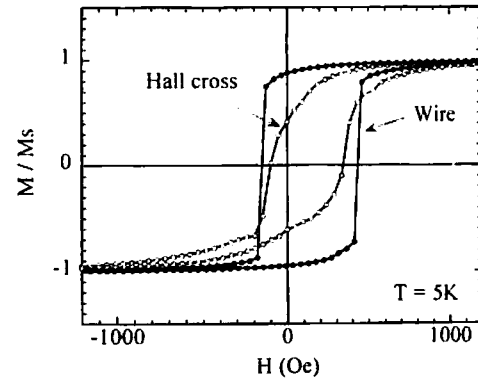


FIG. 3. Magnetic hysteresis loops obtained from magnetoresistivity and planar Hall resistivity measurements in Fig. 2. Solid and open circles represent curves for the wire and in the Hall cross, respectively.

$-\theta_j)/4a^2W$ , where  $J$  is the exchange integral of the ferromagnet and  $a$  is the lattice constant. The magnetic hysteresis loops were calculated by minimizing the total magnetic energy given by a sum of the unidirectional magnetic anisotropy, the uniaxial magnetic anisotropy, the magnetostatic, the exchange, and the Zeeman energies. The unidirectional anisotropy constant of  $1.2 \times 10^5$  erg/cm<sup>3</sup> was determined as  $M_F H_{ex}$  by using the values,  $M_F = 800$  G and  $H_{ex} = 150$  Oe. The uniaxial anisotropy constant of  $9.0 \times 10^4$  erg/cm<sup>3</sup> and the exchange integral of  $3.5 \times 10^{-14}$  erg were determined from the magnetization curve for hard direction and the Curie temperature of the bilayer films prepared under the same condition.

The hysteresis loops obtained from the numerical calculation are in good agreement with the experimental loops in Fig. 3. Detailed magnetization reversal processes are illustrated in Fig. 4(b). First, the magnetization begins to rotate in a voltage lead in order to reduce magnetostatic energy. The magnetization reversal then occurs in the cross, leading to the domain wall nucleation at the boundary between the cross and the wire. The nucleated domain walls propagate throughout the wire and the magnetization reversal is complete. This calculation implies that the magnetization reversal in the cross takes place *via* a coherent rotation. The Hall

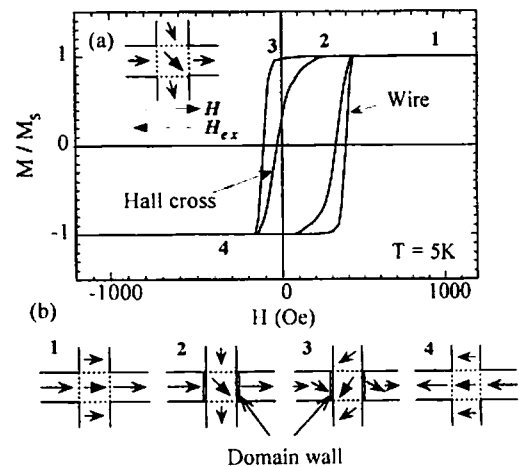


FIG. 4. (a) Hysteresis loops obtained by a numerical simulation. (b) A schematic explanation of a magnetization reversal process determined by the numerical simulation. The numbers in (b) correspond to those indicated in (a).

cross may thus be regarded as a unit exchange coupled area.

By applying the random field approximation<sup>5</sup> and assuming the presence of a cylindrical antiferromagnetic domain with a diameter  $L$ , the interfacial energy  $\sigma(L)$  can be expressed as a sum of the exchange energy at the interface and the antiferromagnetic domain wall energy,

$$\sigma(L) = -\frac{2f_i J_i}{\sqrt{\pi}aL} + \frac{8t_A \sqrt{AK}}{L} \sqrt{1 + \left(\frac{2S\delta_A}{\pi L}\right)^2}, \quad (1)$$

where  $f_i$  is the structural parameter of order unity,  $J_i$  is the microscopic exchange integral at the interface,  $a$  is the lattice constant,  $A$  is the antiferromagnetic exchange stiffness constant,  $K$  is the antiferromagnetic anisotropy constant,  $t_A$  is the antiferromagnetic layer thickness,  $\delta_A$  is the antiferromagnetic domain wall thickness, and  $S$  is the winding number of the domain wall. Equation (1) shows that the antiferromagnetic domain tends to expand to the edge of the Hall cross with the size  $W$ . Since the exchange energy in Eq. (1) only changes its sign after the magnetization reversal of the ferromagnetic layer, the change in the interface energy before and after the magnetization reversal  $\Delta\sigma$  gives the exchange coupling field  $H_{ex}$  as

$$H_{ex} = \frac{\Delta\sigma}{2M_F t_F} = \frac{2f_i J_i}{\sqrt{\pi}M_F t_F a W}. \quad (2)$$

Figure 5 shows the experimentally obtained  $H_{ex}$  plotted against the inverse wire width  $W^{-1}$ . It is clear that the exchange field  $H_{ex}$  is proportional to  $W^{-1}$  at all the measured temperatures. This means that the size of the antiferromagnetic domain formed in the Hall cross is well regulated by the wire width  $W$ . The slope at 5 K gives the interfacial exchange integral  $J_i$  of  $2.1 \times 10^{-14}$  erg using the values  $A = 5.0 \times 10^{-7}$  erg/cm,  $K = 3.3 \times 10^4$  erg/cm<sup>3</sup>,  $M_F = 800$  G, and  $t_F = 200$  Å. The value of  $J_i$  is in good agreement with that evaluated from the Néel temperature of NiO.

In conclusion, the magnetization process of the submicron scale exchange-coupled area was successfully examined

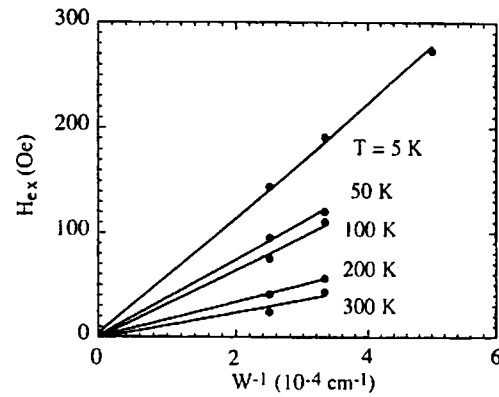


FIG. 5. Exchange coupling field  $H_{ex}$  plotted at various temperatures against  $W^{-1}$ .

by magnetotransport measurements. The magnetization reversal was found to take place *via* coherent rotation in the cross, suggesting the presence of an antiferromagnetic single domain. The magnitude of the exchange coupling field  $H_{ex}$  varied inversely proportional to the wire width.

This work is partly supported by the new energy and industrial technology development organization (NEDO), RFTF of Japan Society for the Promotion of Science, and a Grant-in-aid for Scientific Research from the Ministry of Education, Science, Sports and Culture in Japan.

<sup>1</sup> T. Lin, C. Tsang, R. E. Fontana, and J. K. Howard, IEEE Trans. Magn. 31, 2585 (1995).

<sup>2</sup> H. Uyama, Y. Otani, K. Fukamichi, O. Kitakami, Y. Shimada, and J. Echigoya, Appl. Phys. Lett. 71, 1258 (1997).

<sup>3</sup> J. G. Zhu, Y. Zheng, and X. Lin, J. Appl. Phys. 81, 4336 (1997).

<sup>4</sup> D. Mauri, H. C. Siegmund, P. S. Bagus, and E. Kay, J. Appl. Phys. 62, 3047 (1987).

<sup>5</sup> A. P. Malozemoff, Phys. Rev. B 35, 3679 (1987).

<sup>6</sup> N. C. Koon, Phys. Rev. Lett. 78, 4865 (1997).

<sup>7</sup> W. P. Meiklejohn and C. P. Bean, Phys. Rev. 105, 904 (1957).

<sup>8</sup> J. Nogues, D. Lederman, T. J. Moran, and I. K. Schuller, Phys. Rev. Lett. 76, 4624 (1996).

<sup>9</sup> T. R. McGuire and R. I. Potter, IEEE Trans. Magn. MAG-11, 1018 (1975).